NUMERICAL STUDIES OF DISPERSION AND FLAMMABLE VOLUME OF HYDROGEN IN ENCLOSURES

Zhang, J.[1], Hereid, J.[1], Hagen, M.[1], Bakirtzis, D. [1], Delichatsios, M.A.[1], and Venetsanos, A.G.[2]
[1] FireSERT, University of Ulster, BT37 0QB, UK
j.zhang@ulster.ac.uk
[2] National Center for Scientific Research Demokritos Environmental Research Lab., Greece
venets@ipta.demokritos.gr

ABSTRACT

Hydrogen dispersion in an enclosure is numerically studied using simple analytical solutions and a large-eddy-simulation based CFD code. In simple calculations, the interface height and temperature rise of the upper layer are obtained based on mass and energy conservation and the centreline hydrogen volume fraction is derived from similarity solutions of buoyant jets. The calculated centreline hydrogen volume fraction using the two methods agree with each other; however, discrepancies are found for the calculated total flammable volume as a result of the inability of simple calculations in taking into account local mixing and diffusion. The CFD model, in contrast, is found to be capable of correctly reproducing the diffusion and stratification phenomena during the mixing stage.

1.0 INTRODUCTION

Hydrogen is one of the most promising substitutes of hydrocarbon-based fuels, due to its absence of carbon-based pollutants, the abundance of hydrogen in nature, and the ability to generate hydrogen from sustainable energy sources. The future widespread use of hydrogen demands stringent research on hydrogen safety. The safe design and operation of transportation, high-pressure plant and pipe work require that provision be made for the relief of pressure under certain operational and emergency conditions. Assessments of the consequences associated with accidental releases of flammable material are also needed as the basis of safety reports and risk assessments.

Hydrogen is known to have very low density (about one fourteenth that of air) and wide flammability limit (4-74 vol. %). These unique characteristics imply that hydrogen could disperse extremely fast at an accidental release and combust easily at the presence of an ignition source. A sound understanding of dispersion, stratification and diffusion of accidental hydrogen releases is, therefore, of practical importance and use to better understand the possibility of ignition, combustion and explosion of such releases within the context of hydrogen safety. Towards this end, a series of hydrogen dispersion experiments with several release rates were performed by INERIS within an enclosure with two openings located just above the floor level [1]. In this work, the experiment with a release rate of 1g/s is numerically studied using two independent approaches, i.e. simple analytical calculations and a computational fluid dynamics (CFD) code, fire dynamics simulator (FDS). Cross comparison is made between the results of analytical solutions and CFD predictions and the experimental data, in terms of the hydrogen volume fraction at various locations, the volume flow rate through openings, and the total flammable gas volume.

2.0 PROBLEM DESCRIPTION

The INERIS gallery facility, which was built inside a rock [1], has a shape of a rectangular box (7.2m long × 3.78m wide × 2.88m high). Figure 1 shows the co-ordinate system as well as the locations of the release chamber and two openings. The release orifice has a diameter of 2cm, located at 0.265m above the floor. The two openings with a diameter of 5cm are located at 5cm above the floor. The release mass flow rate is 1g/s, which gives an equivalent exit velocity of around 38m/s. Measurements

were made for hydrogen volume fraction (HVF) using 16 concentration sensors, located on the plane Y=0 as shown in the coordinate system in Fig. 1.

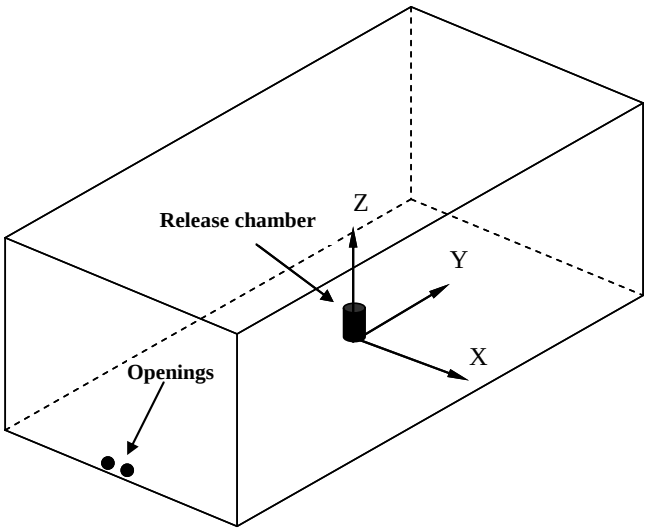

Figure 1. Experimental facility showing the coordinate system and the locations of the release chamber and openings. (Reproduced from [1])

A summary of the locations of the sensors and openings with the x-y-z axes located at the bottom of the release chamber is presented in Table 1. The release lasted 240 seconds; however the recording was up to 7000 seconds to examine the effect of diffusion and stratification.

Table 1. Locations of concentration sensors and openings as shown in the coordinate system in Fig. 1. (Reproduced from [1])

	X (cm)	Y (cm)	Z (cm)
Opening 1 centre location	7.5	-380	7.5
Opening 2 centre location	-7.5	-380	7.5
Sensor 1 location	0	0	283
Sensor 2 location	10	0	283
Sensor 3 location	20	0	283
Sensor 4 location	40	0	283
Sensor 5 location	90	0	283
Sensor 6 location	185	0	283
Sensor 7 location	140	0	283
Sensor 8 location	140	0	268
Sensor 9 location	140	0	238
Sensor 10 location	140	0	188
Sensor 11 location	140	0	138
Sensor 12 location	140	0	88
Sensor 13 location	0	0	268
Sensor 14 location	0	0	238
Sensor 15 location	0	0	188
Sensor 16 location	0	0	138

3.0 ANALYTICAL SOLUTIONS

The analytical solutions were originally developed for predicting smoke filling [2, 3]. The analytical solutions are based on a two-layer zone model subdividing the whole domain into an upper layer of hydrogen and a lower layer of air as schematically shown in Fig. 2. The interface height between hydrogen and air and the temperature rise at the upper layer are obtained based on mass and energy conservation. The HVF along the centreline is calculated from similarity solutions of buoyant jets. The mathematical formulations of the zone model are presented in this section.

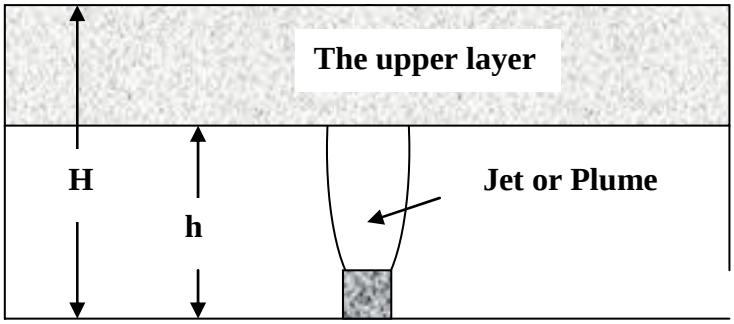

Figure 2. A schematic view of the analytical solutions.

3.1 Mathematical formulations

The conservation equation for the mass balance results in the decrease of the height of the cold air as air is forced to flow out of the enclosure by released hydrogen. For an orthogonal enclosure, mass conservation takes the form [2, 3]:

$$A\frac{dh}{dt} = -0.21\left(\frac{\dot{Q}g}{\rho_o c_p T_o}\right)^{1/3} h^{5/3} - \frac{\dot{Q}(1-\lambda)}{\rho_o c_p T_o} \tag{1}$$

where h – the clear layer height, m; A – the floor area, m^2; t – time, s; g – gravitation acceleration, m/s^2; $\dot{Q}$ – the convective heat release rate (HRR), kW; ρ_o – ambient density, kg/m3; c_p – specific heat, J/kg-K; T_o – ambient and lower layer temperature, K; λ – the fraction of HRR lost by convection to walls and is taken as zero in the present study.

The energy balance is an enthalpy balance for the upper layer, yielding the temperature in the upper layer [1, 2]:

$$\frac{d}{dt}(\rho_u c_p (T_u - T_o)V_u) = \dot{Q}(1-\lambda) \tag{2}$$

where subscript u denotes values in the upper layer with V_u being the volume of the upper layer.

The conservation equations for mass and energy can be solved in their closed forms as [2, 3]:

$$1 - \frac{h}{H} = \frac{Q(1-\lambda)/(\rho_o c_p T_o AH)}{1 - \exp\left(-\dfrac{Q(1-\lambda)/(\rho_o c_p T_o AH)}{\left(1-\left(\dfrac{1}{1+X}\right)^{3/2}\right)}\right)} \tag{3}$$

$$\frac{T_u}{T_o} = \exp\left(\frac{Q(1-\lambda)/(\rho_o c_p T_o AH)}{(1-(\frac{1}{1+X})^{3/2})}\right) \tag{4}$$

where H denotes the height of the enclosure, and

$$Q = \int_0^t \dot{Q} dt \tag{5}$$

$$X = 0.14\left(\frac{g}{\rho_o cp T_o}\right)^{1/3} \frac{H^{2/3}}{A} \int_o^t \dot{Q}^{1/3} dt \tag{6}$$

The volume flow rate at the openings can be calculated:

$$\dot{V}_e = \frac{\dot{m}_e}{\rho_o} = \frac{\dot{Q}}{\rho_o c_p T_o} = \frac{\Delta\rho}{\rho_o} u_N A_N \tag{7}$$

where $\Delta\rho$ denotes the density difference between hydrogen and air, u_N and A_N are respectively the hydrogen release speed and the area of the orifice. Substituting the respective values into Eq. 7, the total volume flow rate for the two openings is found equal to 0.0111m^3/s.

To derive the centreline HVF, a similarity solution to buoyant jets is employed:

$$\frac{(\Delta\rho/\rho)_c}{(\Delta\rho/\rho)_{cB}} = \frac{(z/L_M)^{2/3}}{(5.8+(z/L_M)^2)^{1/3}} \tag{8}$$

where z denotes the height above the jet orifice, and the transition length from momentum to buoyancy, L_m, is defined as:

$$L_M = \frac{(M_o/\rho_o)^{3/4}}{(B_o/\rho_o)^{1/2}} \tag{9}$$

Buoyancy flux is defined as:

$$B_o = \Delta\rho u_N A_N g \ . \tag{10}$$

For the centreline values for buoyant plumes we have:

$$(\frac{\Delta\rho}{\rho})_{cB} = \frac{\rho_{H2} - \rho_O}{\rho_{H2}} = \frac{\Delta T}{T_o} \tag{11}$$

$$\frac{\Delta T}{T_o}(\frac{z}{L_p})^{5/3} = 9.1 \tag{12}$$

where:

$$L_p = \dot{Q}_c^{*2/5} \text{ and } \dot{Q}_c^* = \dot{Q}_c/(c_p\rho_o T_o\sqrt{g}) \tag{13}$$

3.2 Analytical results and discussions

Figure 3 depicts the histories of the normalised height of the clear layer, h/H, and temperature rise at the upper layer, $(T_u - T_o)/T_o$. It is clearly shown that the clear layer height decreases quickly with time as expected and that at 240s the clear layer height is only about 28% of its initial height. The temperature rise, in contrast, increase almost linearly with time. Note these results apply to the whole upper layer, which has uniform properties.

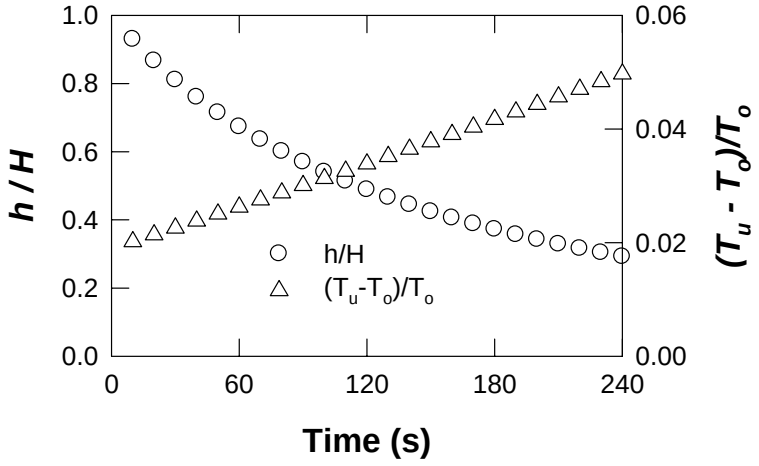

Figure 3. Calculated normalised clear layer height and temperature rise at the upper layer using simple calculations.

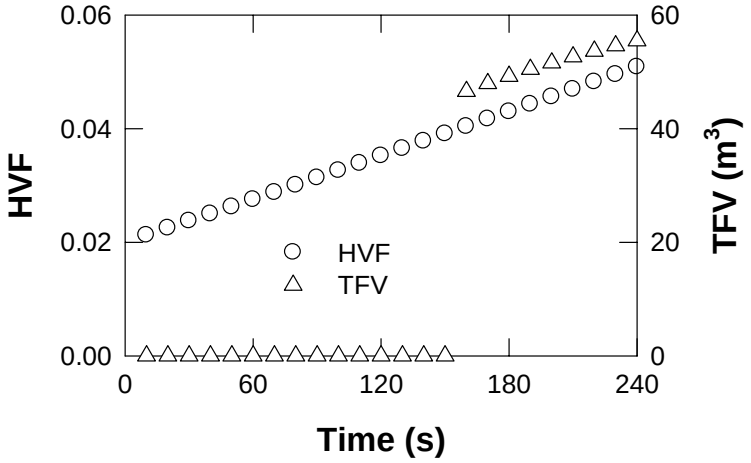

Figure 4. Calculated HVF at the upper layer and the total flammable volume (TFV) using simple calculations.

Based on the interface height and the temperature rise at the upper layer, the density and consequently the HVF at the upper layer can be deduced. The results is presented in Fig. 4, along with the total flammable volume (TFV), i.e. the volume with the HVF within the lower flammability limit (LFL) and upper flammability limit (UFL) – respectively 4% and 70% for hydrogen. The centreline HVF has a similar trend to the temperature rise, which is characterised by a nearly linear increase. For the result of the total flammable gas volume, we note at about 150s a sudden increase from a near-zero value to a value more than 40m3. As hydrogen was released in a continuous manner, this sudden increase is

unrealistic. To explain this unrealistic sudden increase, it is worth recalling that simple calculations are derived based on the assumption that each zone has uniform properties, which has ignored local diffusion and mixing within each zone. From Fig. 4, we note that the HVF at the upper layer exceeds 4%, the LFL, at around 150s, corresponding to when the sudden increase of the TFV occurs.

Figure 5 presents the HVF at the four locations along the centreline, corresponding to the locations of concentration sensors 13, 14, 15 and 16. As mentioned earlier these values were derived from the similarity solution of buoyant jets. These values represent the ones at the steady stage. As expected, the HVF decreases with height. Specifically, a value of 0.16 is found at location 16, 1.38m above the floor, which decreases to 0.05 at location 13, 2.68m above the floor.

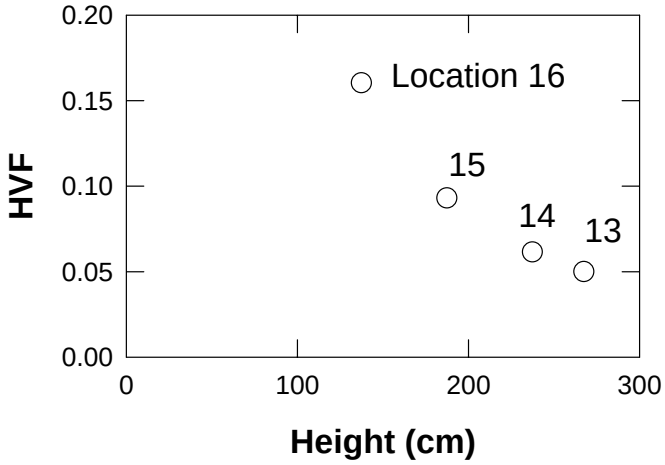

Figure 5. Calculated HVF at centreline using simple calculations.

4.0 CFD MODELLING

4.1 CFD Model description and numerical details

The large-eddy simulation (LES) based CFD code, fire dynamics simulator (FDS), originally developed at NIST [4] for simulations of fire-related phenomena, is used in this study. It employs the finite-difference method, with 2nd order explicit predictor-corrector time discretisation and 2nd order central difference space discretisation. The time-step is determined dynamically during calculations based on the local control volume (CV) size and velocity to ensure computational convergence. A total of about 0.4 million structured CVs is used, with local refinement at the jet centre to capture large gradients of velocity and HVF. Grid sensitivity tests showed that further refinement of the grid size has negligible effect on the simulation results. Calculations were undertaken on a PC with a 3.60GHz dual processor and 3GB of RAM, and the CPU time was about 200 hours. The Smagorinsky constant in the LES model was found to have an important effect on the simulation results—a value of 0.2 commonly-used for fire applications produced significant underprediction of turbulent mixing and eddy formation, and therefore significantly overpredicted HVF. A comparison of the centreline HVF between the experimental data, analytical solution, and FDS solutions with different Smagorinsky constants is shown in Table 2. Clearly, a value of 0.12 could yield results that are in good agreement with the experimental data and analytical solution and thus is used in the current study.

Table 2. Comparison of centreline HVF between the experimental data, analytical solution, and FDS solutions with different Smagorinsky constants.

Sensor	Exp.	Analytical	FDS	FDS

location	(average)	solution	(Cs=0.2)	(Cs=0.12)
13	0.16	0.16	0.39	0.158
14	0.075	0.092	0.32	0.095
15	-	0.062	0.25	0.068
16	0.07	0.05	0.2	0.065

4.2 CFD results and discussions

Figure 7 shows the predictions of the volume flow rates at the two openings using FDS. It is seen that the volume flow rate reaches a constant value after about 20s from the initial release. The steady state values for the two openings are very close, about 0.0055m3/s. Recall that the calculated total volume flow rate for the two openings using analytical solutions in Eq. 7 is equal to 0.0111m3/s. There is a very good agreement between the results of the two approaches.

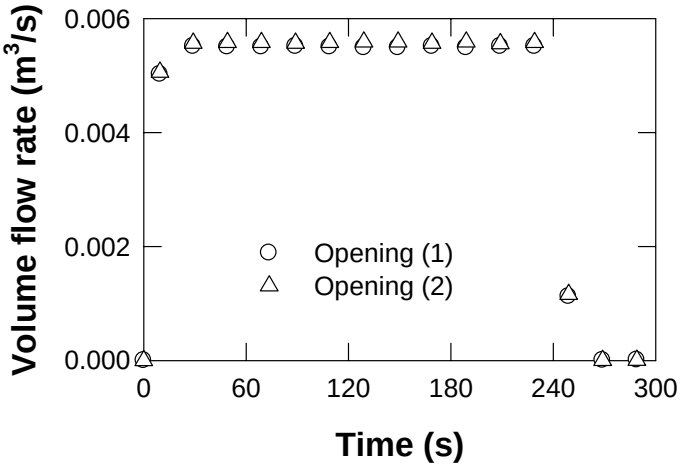

Figure 7. Calculated volume flow rates at the two openings using FDS.

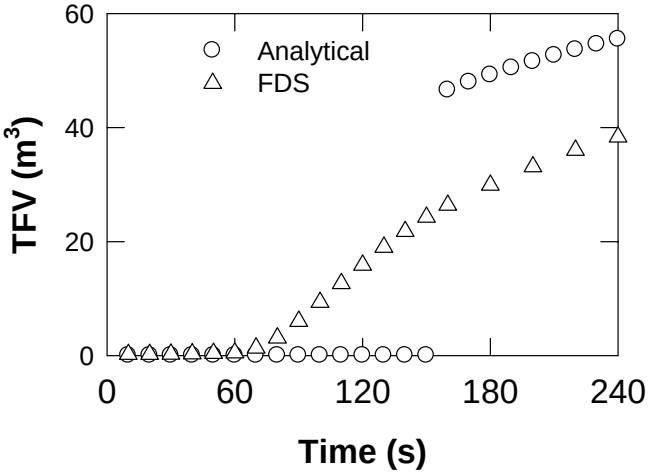

Figure 8. Comparisons of the calculated total flammable volume using simple calculations and FDS.

The TFV in the FDS calculations were obtained by summation of the control volumes having a HVF between the LFL and UFL. The calculated TFV by FDS is compared in Fig. 8 with the one obtained

by simple calculations. From the FDS calculations, it is seen that flammable gas forms after about 70s, while the simple calculations at about 150s. The comparison demonstrates that a detailed CFD analysis is essential for correct understanding of the formation of the flammable gas by accounting for local diffusion and mixing within each zone. Another noticeable difference between the two set of data is that after 150s the predicted flammable gas volume using FDS is much smaller than the one from simple calculations. The overestimation by simple calculations could be attributed again to the assumption of uniform properties in each zone in simple calculations. Another important result is that at 240s the total flammable volume from FDS calculations is about 38m3, which yields the height , above which combustible gas exists, equal to 2.88–38/27.126 = 1.48m. This is an important parameter for safety design as an ignition source above this height could ignite the flammable gas at the upper layer.

The predicted instantaneous snapshots of the HVF at various time instants are presented in Fig. 9. The minimum value shows in the figure corresponds to the LFL. It can be seen that hydrogen impinges on the ceiling, and spreads along the ceilings, and moving downwards upon impacting on the side walls. Prior to 240s there is a core with high concentration hydrogen at the centreline. After the hydrogen supply was ceased at 240s, this core gradually disappears as a result of mixing and diffusion. At 500s the upper layer mixes rather uniformly and stratifies forming two distinctive regions.

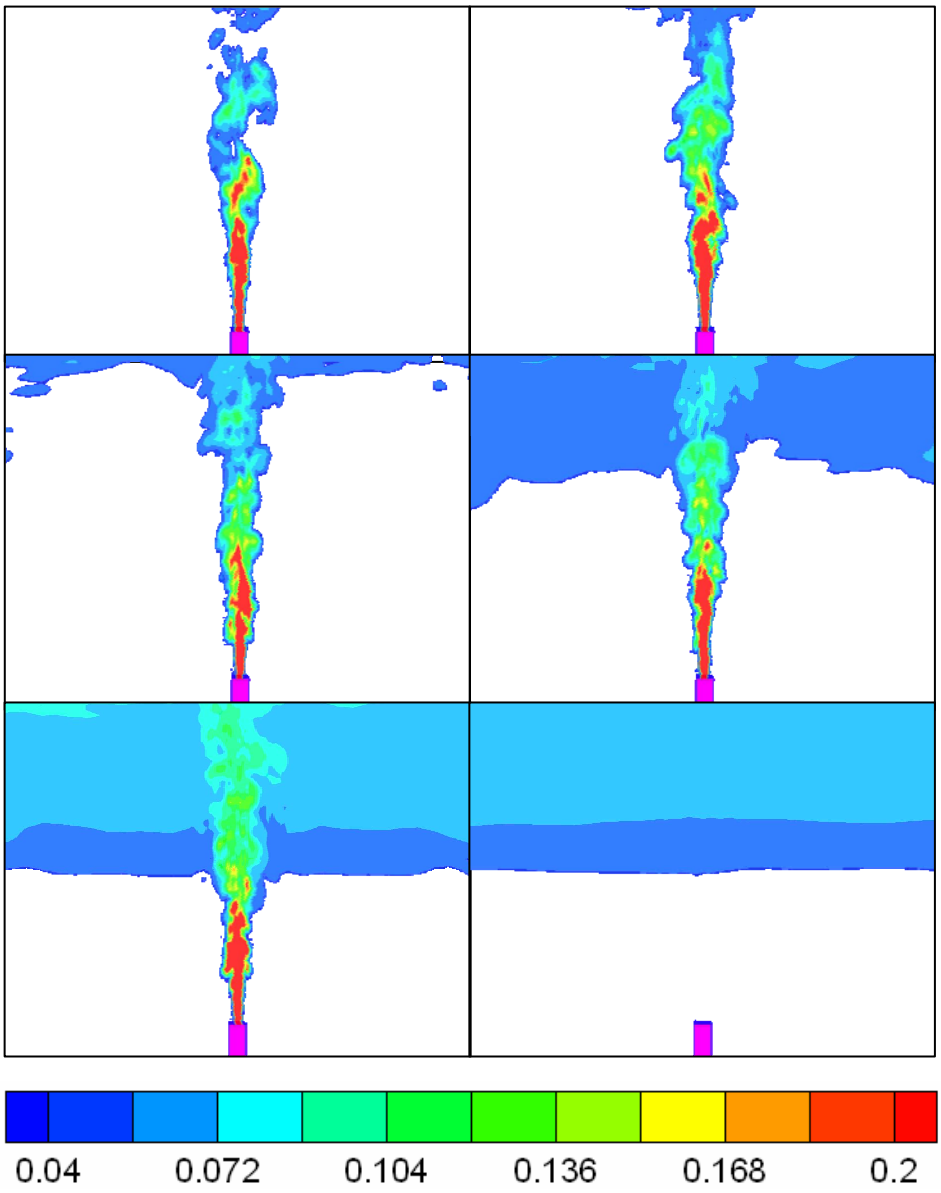

Figure 9. Calculated instantaneous snapshots of HVF using FDS at different time instants (from top left: 10s, 50s, 100s, 150s, 240s and 500s).

Figure 10 shows the comparisons of the HVF between the FDS calculations and experimental data at different locations—Fig. 10a is for locations 1, 4, 6 and 7 located along the ceiling, Fig. 10b for locations 13, 14, 16 along the centreline and Fig. 10c for locations 10 and 11 along the side wall. The FDS predictions generally agree with the experimental data. At the ceiling, the HVF increases with time and reaches its peak at 240s when hydrogen supply is stopped, after 240s hydrogen mixes through diffusion and the HVF eventually becomes constant, about 0.07, slightly lower than the experimental value, about 0.08. The centreline data in Fig. 10b shows that at location 16 FDS predicts a nearly constant value of 0.16, which compares very well with the experimental result and also with the analytical solution. At location 13, HVF increases gradually from 0.05 to 0.08 and at Location 14 from 0.06 to 0.09. Some peaks are observed as a result of the resistance of air at the jet front during the initial release. As previously discussed, after the hydrogen supply is stopped, hydrogen at the upper layer will diffuse to the lower layer, which causes the HVF at the upper layer to decrease and the HVF at the lower layer to increase. Figure 10c, which shows the comparisons of FDS calculations and experimental data at locations 11 and 12, confirms experimentally and numerically this phenomenon.

The comparisons also show a very good quantitative agreement between the two sets of data. At location 12, the HVF is nearly zero before 240s, however it increases quickly with time due to diffusion and reaches a value around 0.009 at 2000s; in contrast at location 11 the HVF increase with time before 240s, after which it slowly decrease with time.

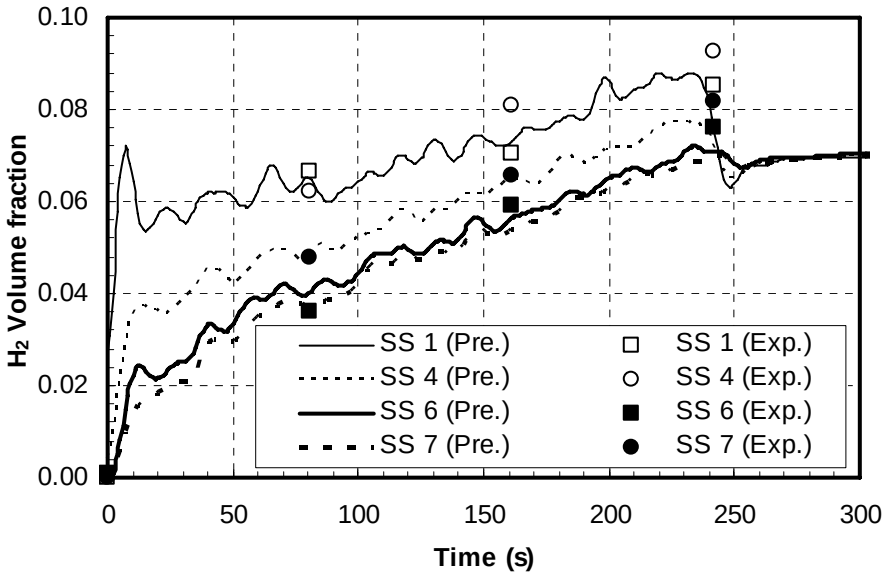

Figure 10a. Comparisons of the HVF between FDS calculations and experimental data at locations 1, 4, 6 and 7.

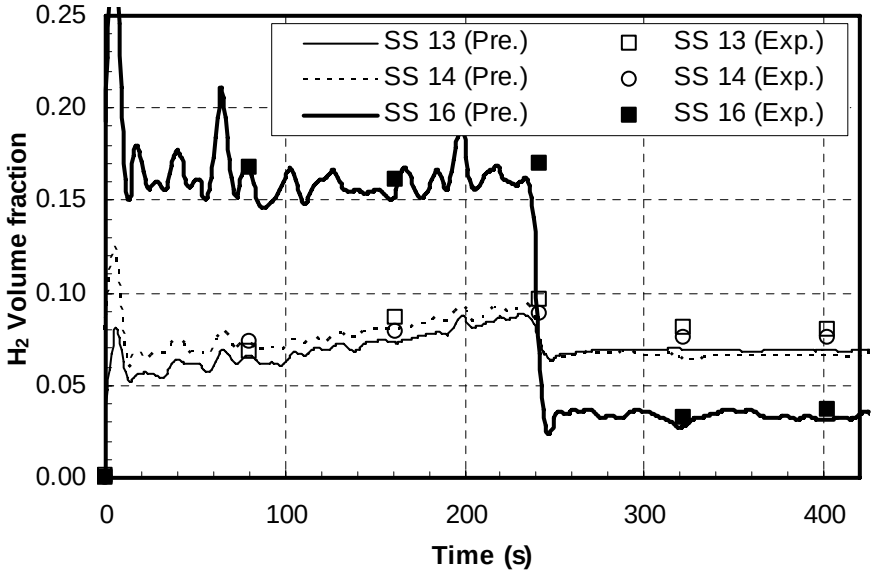

Figure 10b. Comparisons of the HVF between FDS calculations and experimental data at Location 13, 14 and 16.

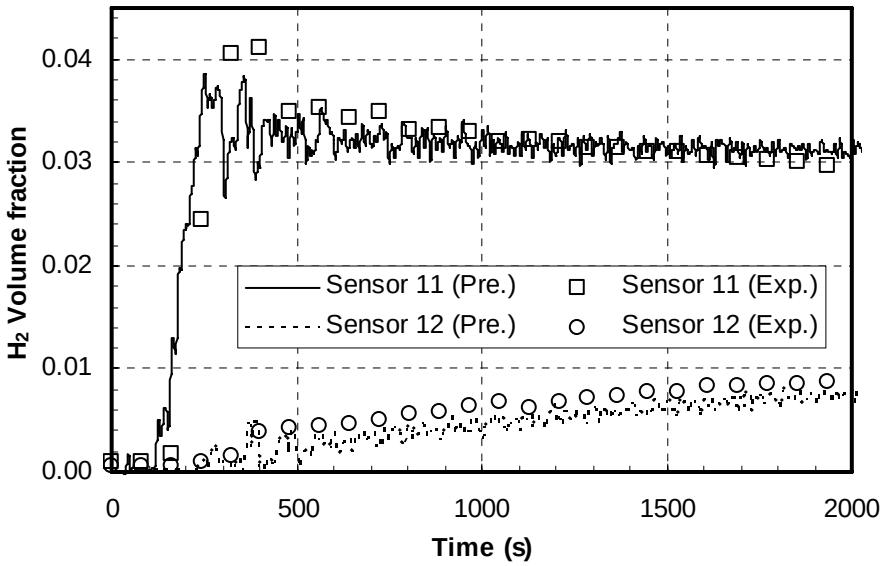

Figure 10c. Comparisons of the HVF between FDS calculations and experimental data at locations 11 and 12.

5.0 CONCLUSIONS

Hydrogen dispersion within an enclosure was numerically studied using simple calculations and a LES based CFD code. Some important conclusions of this study are:

- The analytical solutions, which can be carried out using spreadsheets, provides a simple and efficient means for studying dispersion problems, whereas the CFD model requiring significant computation time enabled a more detailed analysis.

- The volume flow rate at openings was found to be independent of time, and both methods yielded consistent values.

- Simple calculations underestimated the total flammable value before the hydrogen volume fraction at the upper layer exceeds the LFL and overestimate it afterwards as a result of the assumption of uniform properties within each zone. The CFD model, in contrast, predicted a gradual increase.

- For the centreline HVF, there was a good agreement between the experimental data, analytical solutions and CFD results.

- The CFD model correctly predicted the diffusion process after the hydrogen supply was ceased as observed in the experiment.

REFERENCES

1. HYSAFE-INSHYDE project, Description of INERIS-test-6 experiment and requirements for corresponding blind SBEP in the framework of the InsHyde internal project, INERIS and NCSRD, 24/10/2005.
2. Delichatsios, M. A., Closed form approximate solutions for smoke filling in enclosures including the volume expansion term, *Fire Safety Journal,* **38**, 2003, pp. 97-101.

3. Delichatsios, M. A., Tenability conditions and filling times for fires in large spaces, *Fire Safety Journal,* **38**, 2004, pp. 643-662.
4. McGrattan, K. and Forney, G., Fire Dynamics Simulator (Version 4) User's Guide, NISR Special Publication 1019, 2005.